

**Multipair-free source of entangled photons in the solid state**

Julia Neuwirth<sup>1,\*</sup>, Francesco Basso Basset<sup>1,†</sup>, Michele B. Rota<sup>1</sup>, Jan-Gabriel Hartel<sup>2</sup>, Marc Sartison<sup>2</sup>,  
Saimon F. Covre da Silva<sup>3</sup>, Klaus D. Jöns<sup>2</sup>, Armando Rastelli<sup>3</sup>, and Rinaldo Trotta<sup>1,‡</sup>

<sup>1</sup>*Department of Physics, Sapienza University of Rome, Piazzale Aldo Moro 5, 00185 Rome, Italy*

<sup>2</sup>*Institute for Photonic Quantum Systems, Center for Optoelectronics and Photonics, and Department of Physics,  
Paderborn University, Warburger Straße 100, 33098 Paderborn, Germany*

<sup>3</sup>*Institute of Semiconductor and Solid State Physics, Johannes Kepler University Linz, Altenbergerstraße 69, 4040 Linz, Austria*

 (Received 15 April 2022; revised 6 September 2022; accepted 13 September 2022; published 8 December 2022)

We investigate the effect of multiphoton emission on polarization-entangled photon pairs from a coherently driven quantum dot by comparing quantum state tomography and second-order autocorrelation measurements as a function of the excitation power. We observe that the relative (absolute) multiphoton emission probability is as low as  $p_m = (5.6 \pm 0.6) \times 10^{-4}$  [ $p_2 = (1.5 \pm 0.3) \times 10^{-4}$ ] at the maximum source brightness, with a negligible effect on the degree of entanglement. In contrast with probabilistic sources of entangled photons, the multiphoton emission probability and the degree of entanglement remain practically unchanged against the excitation power over multiple Rabi cycles, while observing oscillations in the second-order autocorrelation function by more than one order of magnitude. Our results, explained by a model which links the second-order autocorrelation function to the actual multiphoton contribution in the two-photon density matrix, highlight that quantum dots can be regarded as a multipair-free source of entangled photons in the solid state.

DOI: [10.1103/PhysRevB.106.L241402](https://doi.org/10.1103/PhysRevB.106.L241402)

Entangled photon sources find numerous quantum computation and communication applications and are key ingredients for developing photonic quantum networks [1]. The state of the art is represented by sources based on spontaneous parametric-down-conversion (SPDC) [2] which provides nearly maximally entangled photons, yet with a nonzero probability of emitting more than one entangled photon pair per excitation pulse [3]. When enhancing the brightness, the multipair emission probability also increases, impairing the entanglement fidelity [4]. This limits the technological potential of SPDCs, e.g., it reduces the achievable secure key rate in quantum key distribution [5,6] and hampers the scalability of multiple photon experiments [2]. Solid-state-based quantum emitters, notably epitaxial quantum dots (QDs), have the potential to overcome this hurdle and promise near-deterministic generation of strongly polarization-entangled photons via the biexciton-exciton cascade [7,8]. In principle, this comes with no compromise between multiphoton emission and brightness [9,10], improving current applications [11]. However, the presence of reexcitation effects has often been reported [12,13], with experimental evidence that the degree of entanglement depends on the finite values of  $g^{(2)}(0)$ , which vary as a function of the excitation power [14]. On the one hand, these experiments do not employ resonant excitation, and it is often experimentally challenging to ascertain whether the entanglement degradation and the finite  $g^{(2)}(0)$  values are due to true multiphoton emission or background light originating

from the excitation laser and/or states not involved in the entangled photon generation process. On the other hand, it is known that even for coherently driven two-level systems reexcitation processes in QDs can lead to non-negligible values of the second-order autocorrelation function  $g^{(2)}(0)$  [as measured via a Hanbury Brown and Twiss (HBT) interferometer], especially when values of excitation power beyond the optimal brightness condition are employed [15]. This effect is much less pronounced for photons emitted from the biexciton-exciton radiative cascade, provided that the laser pulse length is sufficiently short [16,17]. Nonetheless, these experimental studies did not investigate the degree of entanglement of the emitted photon pairs. Therefore, it remains unclear whether the biexciton-exciton cascade in QDs can be practically regarded as a multipair-free source of polarization-entangled photons. This Letter provides a positive answer to this question by carefully looking at the interplay between second-order coherence, multiphoton emission, and degree of entanglement in resonantly driven QDs. We discuss the presence in the literature [14,18] of conflicting formulas that relate the information on multipair emission given by the  $g^{(2)}(0)$  to the polarization density matrix. We argue that the effect of multiphoton emission on the experimental density matrix is quantified by the fraction of emission events in which more than one photon pair is generated ( $p_m$ ). This quantity is inferred from the autocorrelation function and from the pair production probability measured in the same setup, without the need for modeling the specific physical mechanism that generates the multiple photon pairs. Establishing the relationship between the experimentally determined density matrix and the autocorrelation function requires specific knowledge about blinking and the efficiency in initiating the

\*julia.neuwirth@uniroma1.it

†francesco.bassobasset@uniroma1.it

‡rinaldo.trotta@uniroma1.it

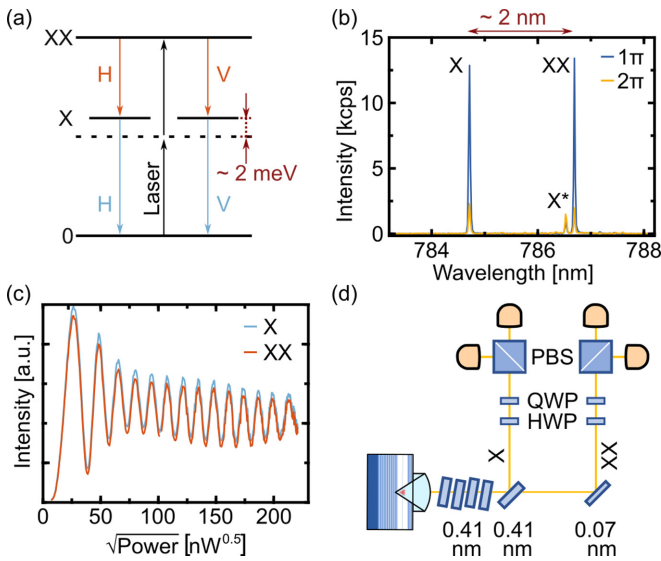


FIG. 1. (a) Resonant two-photon excitation of the XX-X cascade. (b) Photoluminescence spectrum of the QD at  $\pi$  and  $2\pi$  pulse. A line ( $X^*$ ) unrelated to the cascade is observed. (c) Rabi oscillations of X/XX emission intensity vs laser power. Note that these measurements were performed on a different QD. (d) Quantum state tomography setup. The laser is filtered by volume Bragg gratings. X and XX are spectrally filtered with bandwidths of 0.41 and 0.07 nm, respectively. For the second-order autocorrelation measurements, the PBSs are exchanged with 50:50 BSs.

biexciton-exciton cascade. We finally show that, under given resonant two-photon excitation conditions, with a short laser pulse duration compared to the lifetimes of the optical transitions, the relative multiphoton emission probability  $p_m$  is negligible and varies marginally with respect to the excitation power, leading to constant entanglement figures of merit over multiple Rabi cycles.

We use GaAs/AlGaAs QDs grown by droplet etching epitaxy [19,20]. These nanostructures provide state-of-the-art fidelity to a maximally polarization-entangled state without resorting to spectral or temporal selection [21]. The sample design, described in Ref. [22], uses a planar cavity and a solid immersion lens to achieve an extraction efficiency at the first lens of about 10%. The sample is operated at 4 K in a closed-cycle cryostat and driven by a Ti:sapphire laser with a repetition rate of 80 MHz and a pulse duration—adapted with a pulse slicer—of approximately 10 ps. The laser is tuned to half the energy difference between the biexciton (XX) and the ground state (0) to achieve resonant two-photon excitation [23,24], as illustrated in the energy scheme in Fig. 1(a). The mismatch between the laser energy and the emission energies of the exciton (X) and the XX state, due to a XX binding energy of about 4 meV (wavelength of about 2 nm), allows for spectral filtering of the laser back-reflection. Emission spectra for two different pump powers and pair generation rates are shown in Fig. 1(b). The two peaks with higher intensity correspond to the two transitions of the XX-X cascade, whereas the secondary peak ( $X^*$ ) is unrelated to the cascade and has a linear dependence on the laser power [17]. Focusing on the X and XX lines, Fig. 1(c) shows a typical excitation power dependence of their integrated intensity, with Rabi oscillations

reflecting the coherent excitation of a three-level system. Different from the coherent excitation of a two-level system, the oscillations are not a periodic function of the square root of the excitation power, as in two-photon excitation the oscillation period strongly depends on the pulse shape and the biexciton binding energy [24]. A weak continuous-wave off-resonant light field is added in excitation to maximize the “on” time of the QD [21]. This method, known as photoneutralization [25], partially counters the presence of blinking, namely extra charges transiently trapped in the QD and inhibiting the two-photon absorption process. Arguably, the nonresonant field randomly creates charges that can be trapped inside the QD and change its occupation state. It can be adjusted in intensity to optimize the probability that the QD sits in its ground state, where it can be successfully excited by two-photon absorption. Complete blinking suppression can be achieved by placing the QD in an *n-i-p* diode structure [26,27]. Finally, we selected a QD with a fine structure splitting lower than the spectral resolution of  $0.5 \mu\text{eV}$ . This minimizes the induced relative phase precession in the polarization-entangled state [28].

The experimental setup is sketched in Fig. 1(d). Volume Bragg gratings with 0.41-nm bandwidth are placed to remove scattered laser light and background emission. The X and XX are spectrally separated using filters with bandwidths of 0.41 and 0.07 nm, respectively. Note that the XX filter bandwidth is chosen narrower to remove the undesired  $X^*$  peak, but both bandwidths are large enough not to filter out any significant fraction of the signal from the X and XX states. The rest of the setup performs polarization-resolved coincidence measurements between XX and X photons. It consists of two sets of a half wave plate and a quarter wave plate (for state rotation), a polarizing beam splitter (PBS, for state projection), and two avalanche photodiodes (APDs). When measuring  $g^{(2)}(\tau)$  of the X and XX emission, each PBS is replaced with a 50/50 beam splitter (BS), as in a standard HBT interferometer.

Using the HBT setup, we measured  $g^{(2)}(\tau)$  for different excitation powers. Figure 2(a) shows, in logarithmic scale, the coincidence histograms for the X at the  $\pi$ - and  $2\pi$ -pulse area. The  $g_X^{(2)}(0)$ , defined as the coincidences of photons generated with the same laser pulse (zero-time delay) normalized by that of an equally bright Poisson distributed source, is  $(3.4 \pm 0.4) \times 10^{-3}$  at peak brightness  $\pi$  pulse.

To compare this value with the literature, we normalize the coincidences at zero-time delay to the coincidences at consecutive excitation laser pulses (12.5 ns time delay), as done in Fig. 2(a). This leads to  $\tilde{g}_X^{(2)}(0) = \eta_{\text{blink}} g_X^{(2)}(0) = (1.0 \pm 0.1) \times 10^{-3}$ , which is lower by a factor  $\eta_{\text{blink}} = 0.29$ , attributed to the blinking of the source (see Supplemental Material for  $g^{(2)}$  normalization, Sec. I [29]). The value we obtain is very similar to those reported for the GaAs/AlGaAs system [30], only surpassed by the record value obtained using single-photon detectors with ultralow dark count rates [17]. However, we emphasize that the figures reported here are achieved without polarization suppression of the laser back-reflection or postselection schemes.

Figure 2(b) shows how  $g^{(2)}(0)$  varies with power up to above the  $5\pi$ -pulse area. The values obtained for the X and XX lines are compatible within the margin of error (assuming a Poisson distribution of the coincidence counts).

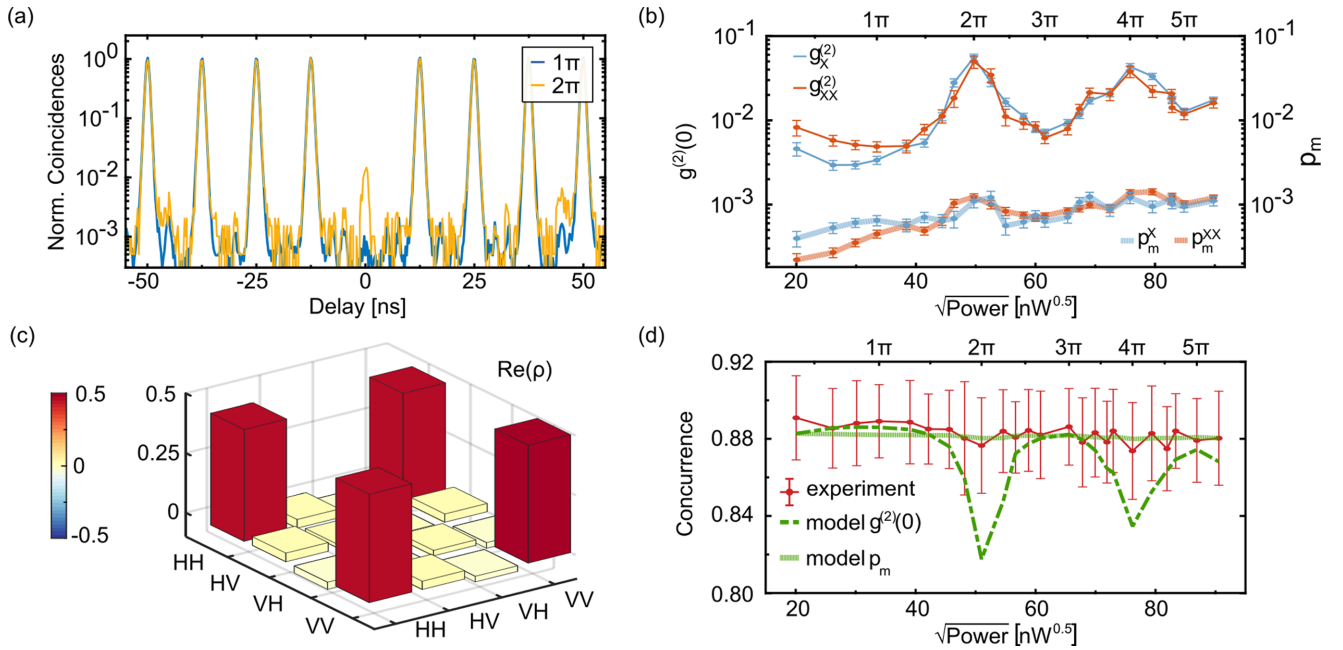


FIG. 2. (a) Second-order autocorrelation function  $\bar{g}_X^{(2)}(\tau)$ , normalized to the side peaks (12.5 ns), at  $\pi$ - and  $2\pi$ -pulse area. (b) Measured  $g^{(2)}(0)$  and multiphoton probability  $p_m$  from the X and XX lines for different excitation powers.  $g^{(2)}(0)$  increases at even  $\pi$ -pulse areas in contrast to  $p_m$ . (c) Real part of the density matrix of the XX-X photon polarization state measured at  $\pi$ -pulse area. (d) Concurrence for different excitation powers. Experimental data (red) are compared with the predictions of Eqs. (1) and (2) (dashed green line) and Eq. (5) (our model, continuous green line). The error bars in the modeled values, estimated from the measured multiphoton probability using a Monte Carlo simulation, are within the line thickness.

Clear maxima up to  $(55.9 \pm 5.1) \times 10^{-3}$  are observed at even  $\pi$ -pulse areas. Similar oscillations have been experimentally observed in QDs [15], though only in resonantly driven two-level systems (2LSs), in which the maxima stem from increased multiphoton emission. Specifically, the 2LS can spontaneously decay to the ground state instead of undergoing an even number of  $\pi$  rotations. In this case, if the excitation laser pulse is still present, a second excitation is possible [15]. This breaks the even  $\pi$ -pulse area excitation into two uneven  $\pi$ -pulse area excitations with a radiative recombination in between. While for cascaded quantum ladder systems reexcitation is expected to be strongly suppressed [17]—as it can take place only when both the X and XX photons are emitted—the oscillations observed in Fig. 2(b) may indicate that the multiphoton emission probability is non-negligible and oscillates with power. To show that this is not the case, we use an approach that does not rely on any assumption on the physical origin of the multiphoton emission. We infer its contribution from the experimental  $g^{(2)}(0)$  of the photons emitted by the XX-X cascade and investigate its effect on the measured degree of entanglement, as discussed below.

We perform polarization-resolved XX-X cross-correlation measurements to reconstruct the two-photon density matrix using the setup from Fig. 1(d). Rotations in the polarization state induced by optical components are compensated for by using a set of linear wave plates to maximize the fidelity to the expected Bell state  $|\phi^+\rangle$  [31]. The density matrix is reconstructed from 36 correlation measurements using quantum state tomography and maximum likelihood estimations [32].

Figure 2(c) shows the resulting real part of the density matrix at the  $\pi$ -pulse area. The imaginary part does not contain significant terms (no matrix element is above 0.045 in absolute value). Furthermore, the fidelity to  $|\phi^+\rangle$  is  $(0.93 \pm 0.01)$ , while the concurrence is  $(0.89 \pm 0.02)$ , values that are comparable with similar systems in the literature [30]. It is worth mentioning that higher figures of merit— $(0.978 \pm 0.005)$  fidelity and  $(0.97 \pm 0.01)$  concurrence—have been obtained with strain-tunable QDs [21], a difference which is arguably attributed to dot-dependent decoherence mechanisms [18]. We note that the influence of a nonmeasurable fine structure splitting (below  $0.5 \mu\text{eV}$ ) should affect the fidelity by less than 1% [31]. Additionally, we characterized the wave-plate retardance and detector dark counts and simulated their impact on the density matrix estimation to conclude that their impact amounts to less than 0.7% on the Bell-state fidelity. The error bars are estimated with a Monte Carlo method assuming a Poisson distribution of the coincidence counts.

Quite remarkably, no significant variation of these figures of merit is observed at the  $2\pi$ -pulse area and across the whole range of powers investigated in this work, as shown in Fig. 2(d). This result is in stark contrast with the behavior of SPDC entangled photon sources [2]. Furthermore, it implies that any multiphoton emission whose presence is associated with the nonzero  $g^{(2)}(0)$  values reported in Fig. 2(b) negligibly affects the degree of entanglement. In general, the measured entanglement is degraded by erroneous detection events of an X and XX photon belonging to different photon pairs from subsequent (thus uncorrelated) cascades. Multiphoton components have been included in the density matrix  $\rho$  in previous

works using knowledge of the  $g^{(2)}(0)$  in the following way [14,21]:

$$\rho = \frac{1}{4}(1-k)\mathbb{I} + k\rho_0, \quad (1)$$

$$1-k = \frac{1}{2}(g_X^{(2)}(0) + g_{XX}^{(2)}(0)), \quad (2)$$

with  $\rho_0$  being the density matrix neglecting accidentals due to multiphoton components,  $k$  being the fraction of photon pairs that come from a radiative XX-X cascade with respect to the total number of detected pairs. According to this model, a link between concurrence and pulse area should be visible, as indicated by the dashed line in Fig. 2(d), obtained using Eqs. (1) and (2) and the  $g^{(2)}(0)$  measurements reported in Fig. 2(b). The discrepancy is especially evident at even  $\pi$  pulses, which motivates the effort to investigate a wide range of excitation powers.

To address the root of this inconsistency we rely on a probability-based model to estimate how multiphoton emission affects the measurements of  $g^{(2)}(0)$  and  $\rho$ . In fact, the  $g^{(2)}(0)$ , as measured via HBT, can be used to estimate the multiphoton contribution to the density matrix, as long as a factor linked to the different normalization of the two measurements is taken into account.

The multiphoton contribution to the density matrix is most effectively described by the relative multiphoton emission probability  $p_m$ . This parameter corresponds to the probability that a successful cascaded photon emission is followed by reexcitation and a second cascaded photon emission. For simplicity, we exclude multiple emission events beyond double, which are expected to be a negligible fraction in all realistic cases.  $p_m$  is related to the photon generation distribution, where  $p_1$  ( $p_2$ ) is the probability per excitation pulse of generating a single (two) photon pair(s) per transition. Therefore, it does not include losses after the emission process. Using a set of basic probabilities that describe photon generation, collection, and detection, it is possible to estimate the parameter  $k$  that enters the density matrix. In the limit of small setup efficiency (see Supplemental Material for setup losses, Sec. IV [29]), we have (see Supplemental Material for derivation, Sec. II [29])

$$1-k = \frac{2p_m}{1+3p_m}. \quad (3)$$

Here the numerator is proportional to the probability of having a coincidence between a photon emitted by a first XX-X cascade and a second photon coming from reexcitation, which are uncorrelated events and therefore lead to a decreased level of measured entanglement. The denominator is proportional to all the possible coincidence combinations, including entangled photons coming from the same cascade. These correlated coincidences are proportional to  $1+p_m$ , where the two terms correspond to the first and second emitted cascade respectively. Inserting Eq. (3) into Eq. (1), we obtain a formula for the density matrix, which includes the multiphoton contribution as quantified by  $p_m$ .

On the other hand, to relate the  $g^{(2)}(0)$  to  $p_m$  we need to include additional information about the probability of photon generation at the source. Using the same probability-based

model as before, given the overall efficiency of the setup well below unity, we estimate (see Supplemental Material for derivation, Sec. II [29])

$$g^{(2)}(0) = \frac{2p_m}{\eta_{\text{blink}}\eta_{\text{prep}}(1+p_m)^2}, \quad (4)$$

where  $\eta_{\text{prep}}$  is the preparation fidelity, defined as the probability that a laser pulse will result in the emission of a photon pair given the QD is in its active ground state. The term  $\eta_{\text{blink}}\eta_{\text{prep}}$  at the denominator corresponds to the probability of photon emission from the cascade  $p_1+p_2$ , split into two main contributions. Equation (4) is equivalent to  $g^{(2)}(0) = p_2/(p_1+2p_2)^2$ , as follows from the definition of second-order autocorrelation, always under the assumption of negligible multiple emission events beyond double. This matches widely used estimations of upper bounds for multiphoton emission from intensity autocorrelation measurements [33,34].

However, the form of Eq. (4) highlights that the  $g^{(2)}(0)$  depends on  $p_m$ , as for the quantity  $k$ , yet also on an additional term equal to the inverse of the probability of photon pair generation. An intuitive explanation can account for this difference: In autocorrelation measurements, the zero-time delay coincidences are proportional to  $\eta_{\text{blink}}\eta_{\text{prep}}$  and  $p_m$ , whereas the coincidences used for normalization are instead proportional to  $(\eta_{\text{blink}}\eta_{\text{prep}})^2$ . The latter are related to two laser pulses, with a relative delay well beyond the blinking correlation time, successfully exciting the QD. Instead, in quantum tomography, one is only interested in cross-correlation coincidences at zero-time delay, without normalization on coincidences at other time delay. Therefore, the additional term due to  $\eta_{\text{blink}}\eta_{\text{prep}}$  is not present in Eq. (3), which only contains  $p_m$ .

Combining the two formulas allows us to estimate the effect of multiphoton emission on  $\rho$  based on the knowledge of  $g^{(2)}(0)$ . In the limit of a small fraction of multiphoton emission events, which is an excellent assumption for our source, we obtain the following expression:

$$1-k \approx \frac{g_X^{(2)}(0) + g_{XX}^{(2)}(0)}{2} \eta_{\text{prep}} \eta_{\text{blink}} = \frac{\tilde{g}_X^{(2)}(0) + \tilde{g}_{XX}^{(2)}(0)}{2} \eta_{\text{prep}}. \quad (5)$$

Equation (5) does account for different normalization criteria of the second-order correlation function by introducing the appropriate corrective factor. Only  $\eta_{\text{prep}}$  enters the equation if the coincidences for consecutive excitation laser pulses are used for normalization.

To verify the model, we need to estimate  $\eta_{\text{prep}}$ . Since it strongly varies across Rabi oscillations, studying the whole power dependence, even  $\pi$ -pulse areas included, illuminates the role of this variable.  $\eta_{\text{prep}}$  is often inferred from the power dependence of the photoluminescence as in Fig. 1(c), using a model to extract the occupation number of the XX state. Here we opt for a different approach, which requires fewer assumptions and prevents us from neglecting power-dependent blinking dynamics. We estimate  $\eta_{\text{prep}}$  from intensity cross-correlation measurements between X and XX photons [18,35], using the setup of Fig. 1(d) but without polarization selection. The coincidence probability (per laser pulse)

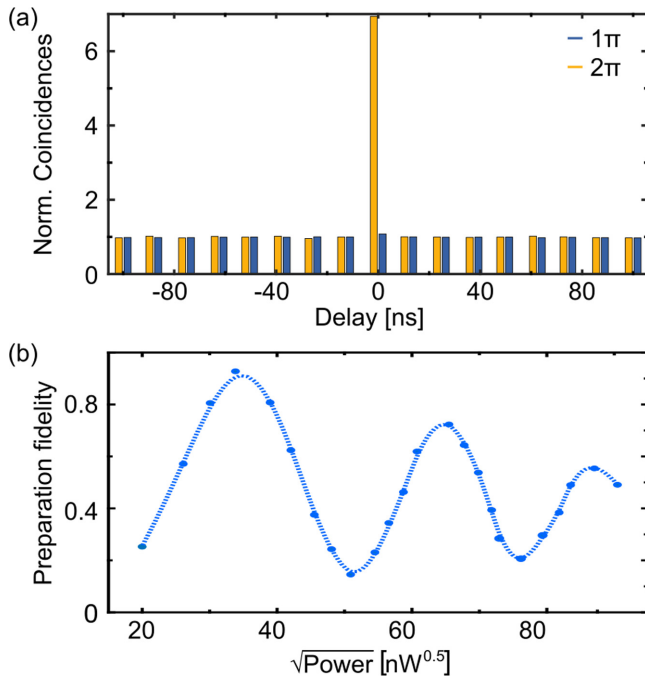


FIG. 3. (a) Coincidence histograms between X and XX photons, normalized to the side peaks (12.5 ns), for  $\pi$ - and  $2\pi$ -pulse area excitation. (b) Measured preparation fidelity (dots) for different pumping regimes, with a spline interpolation to visualize the oscillations as a guide to the eye. The error bars are within the dot size.

divided by the probabilities of individually detecting a X and a XX photon equals the inverse of the photon pair generation probability [36]. In the XX-X cross-correlations histogram, this corresponds to the zero-time delay peak normalized to the ones in the long-time delay limit. As for the autocorrelation histogram, the blinking contribution can be separated, and  $\eta_{\text{prep}}$  is estimated as the inverse of the zero-time delay peak, due to photons from the same cascade, normalized to the side peaks from photons belonging to subsequent excitation pulses. The XX-X cross-correlation histograms normalized to the side peaks (12.5 ns) for  $\pi$ - and  $2\pi$ -pulse areas are shown in Fig. 3(a).  $\eta_{\text{prep}}$  as a function of the pump power is reported in Fig. 3(b), displaying the expected population oscillations, with the highest (lowest) value of 0.93 (0.14) at the  $\pi$ - ( $2\pi$ -) pulse area. The highest preparation fidelity is comparable to those published for similar GaAs/AlGaAs QDs [6].

It is important to emphasize that this method does not require any assumption on how to model the damping of the Rabi oscillations. Moreover, power-dependent changes of  $\eta_{\text{blink}}$  also affect the photoluminescence intensity. They should not be neglected when inferring information about the coherent coupling between ground level and XX state. In our investigated QD, the blinking dynamics show a significant power dependence of its characteristic time [37], ranging 16.1 to 1.6  $\mu\text{s}$  (see Supplemental Material for blinking dynamics, Sec. III [29]). However, while achieving partial photoneutralization adding an off-resonant light field,  $\eta_{\text{blink}}$  is approximately 0.3 in almost the entire interval of pump powers. In general, the behavior of the photoluminescence intensity with excitation power would differ from that of the

preparation fidelity as estimated in Fig. 3(b) by the power-dependent variations in the factor  $\eta_{\text{blink}}$ .

Given these findings, it is apparent from Eq. (3) that the oscillations in the  $g^{(2)}(0)$  are not necessarily related to variations in the multiphoton emission probability but rather to oscillations in the preparation fidelity. Using the measured values of  $g^{(2)}(0)$ ,  $\eta_{\text{prep}}$ , and  $\eta_{\text{blink}}$ , Eq. (3) can be exploited to directly calculate  $p_m$ , without any specific assumption on the physical origin of the multiphoton component. The resulting continuous line in Fig. 2(b) highlights that the fraction of emission events related to multiphoton emission does not noticeably vary with the pump power, i.e.,  $p_m$  slightly varies with the pulse area. This, combined with Eq. (4), readily explains why the oscillations in the  $g^{(2)}(0)$  are not linked to any oscillation of the degree of entanglement with pump power. Moreover, its quantitative contribution appears negligible, at least for the laser pulse width used in this work to drive the two-photon excitation process. At the maximum source brightness ( $\pi$ -pulse area), we estimate that the level of multiphoton emission is  $p_m = (5.6 \pm 0.6) \times 10^{-4}$ , corresponding to an absolute value  $p_2 = (1.5 \pm 0.3) \times 10^{-4}$ . These values applied to an ideal Bell state would result in a concurrence of 99.8%. Having ruled out the effects of multiphoton emission and fine structure splitting, the lower concurrence measured in our experiment is tentatively attributed to cross-dephasing processes in the bright exciton state for this particular QD [18]. Despite that the coherence of the polarization state of the XX-X cascade is expected to be affected only partially and on very short time scales by charge and spin noise, these mechanisms could still cause dot-dependent decoherence [28]. Nonetheless, further studies are required to address residual performance limitations on as-grown solid-state quantum emitters. Ultimately, using Eq. (5) in combination with Eq. (1), where  $\rho_0$  is the density matrix measured at minimum excitation power, we obtain an excellent agreement between our model and the experimental data for the concurrence reported in Fig. 2(d).

In conclusion, we have shown that the effect of multiphoton emission on the degree of entanglement of photons emitted via the biexciton-exciton cascade by resonantly driven QDs is negligible and, contrarily with the behavior reported for single-photon generation in 2LS [38], does not vary significantly with pump power. This occurs while we observe oscillations in the  $g^{(2)}(0)$  by more than one order of magnitude. We illustrate that these variations are not necessarily related to the variation of the multiphoton emission probability, but rather to variations of the preparation fidelity of the excited state. With the support of a probability-based model, we identify the actual contribution of the relative multiphoton emission  $p_m$ , as estimated from the  $g^{(2)}(0)$ , which enters the simulation of the quantum tomography results and successfully reproduces the experimental data.

This work thus tackles a fundamental obstacle for state-of-the-art entangled photon sources based on SPDC: the relationship between pump power, brightness, and entanglement quality. Even though the absence of a tradeoff between brightness and entanglement due to the multiphoton emission has long been a motivation for developing QD-based sources, we finally provide a thorough experimental study demonstrating that multiphoton emission is negligible and does not

negatively affect the generated entangled states across a wide range of excitation powers. The result strengthens the case for QDs providing highly entangled photons for complex quantum information protocols.

The results do not immediately apply to other schemes of entanglement generation, such as for time-bin entangled photons [39] or cluster states [40]. However, it is worth mentioning that the entanglement can also be converted from the polarization to the time-bin degree of freedom [41].

The entanglement fidelity reported in this work was yet below unity, which has been attributed to residual decoherence mechanisms between the bright exciton states [21]. However, the loss of coherence can be significantly lower in selected QDs [21,42]. Additionally, the effect could be further reduced with the help of photonic cavities to shorten the lifetime of the optical transition [43,44] and taking particular care of the length of the pulse used to drive the two-photon excitation process [45]. This approach would reduce the effective interaction time between the exciton spin and environmental factors [43,44,46]. This strategy is predicted to increase the

entanglement fidelity above 0.99 and bring QD entanglement to the same level as SPDC sources [47–49]. Since this performance is achieved without sacrificing brightness due to multiphoton emission, QD-based entangled photon sources will be essential for performing quantum information protocols of ever-increasing complexity.

This project has received funding from the European Research Council (ERC) under the European Union’s Horizon 2020 Research and Innovation Program under Grant Agreement No. 679183 (SPQRel), by the European Union’s Horizon 2020 Research and Innovation Program under Grant Agreements No. 899814 (Qurope) and No. 871130 (Ascent+), by the Austrian Science Fund via the Research Group FG5, I3762, and I4380, by MIUR (ministero dell’Istruzione, dell’Università e della Ricerca) via the PRIN 2017 project, “Taming complexity via Quantum Strategies a Hybrid Integrated Photonic approach (QUSHIP),” Project No. 2017SRNBRK. We thank Radim Filip and Miroslav Ježek for fruitful discussions.

- 
- [1] S. Wehner, D. Elkouss, and R. Hanson, Quantum internet: A vision for the road ahead, *Science* **362**, eaam9288 (2018).
- [2] H.-S. Zhong, Y. Li, W. Li, L.-C. Peng, Z.-E. Su, Y. Hu, Y.-M. He, X. Ding, W. Yang, H. Li *et al.*, 12-Photon Entanglement and Scalable Scattershot Boson Sampling with Optimal Entangled-Photon Pairs from Parametric Down-Conversion, *Phys. Rev. Lett.* **121**, 250505 (2018).
- [3] J. Schneeloch, S. H. Knarr, D. F. Bogorin, M. L. Levangie, C. C. Tison, R. Frank, G. A. Howland, M. L. Fanto, and P. M. Alsing, Introduction to the absolute brightness and number statistics in spontaneous parametric down-conversion, *J. Opt.* **21**, 043501 (2019).
- [4] M. Takeoka, R.-B. Jin, and M. Sasaki, Full analysis of multiphoton pair effects in spontaneous parametric down conversion based photonic quantum information processing, *New J. Phys.* **17**, 043030 (2015).
- [5] R. Hošák, I. Straka, A. Predojević, R. Filip, and M. Ježek, Effect of source statistics on utilizing photon entanglement in quantum key distribution, *Phys. Rev. A* **103**, 042411 (2021).
- [6] F. B. Basset, M. Valeri, E. Roccia, V. Muredda, D. Poderini, J. Neuwirth, N. Spagnolo, M. B. Rota, G. Caravacho, F. Sciarrino *et al.*, Quantum key distribution with entangled photons generated on demand by a quantum dot, *Sci. Adv.* **7**, eabe6379 (2021).
- [7] H. Jayakumar, A. Predojević, T. Huber, T. Kauten, G. S. Solomon, and G. Weihs, Deterministic Photon Pairs and Coherent Optical Control of a Single Quantum Dot, *Phys. Rev. Lett.* **110**, 135505 (2013).
- [8] C. Schimpf, M. Reindl, F. Basso Basset, K. D. Jöns, R. Trotta, and A. Rastelli, Quantum dots as potential sources of strongly entangled photons: Perspectives and challenges for applications in quantum networks, *Appl. Phys. Lett.* **118**, 100502 (2021).
- [9] A. Predojević, M. Ježek, T. Huber, H. Jayakumar, T. Kauten, G. S. Solomon, R. Filip, and G. Weihs, Efficiency vs. multiphoton contribution test for quantum dots, *Opt. Express* **22**, 4789 (2014).
- [10] N. Somaschi, V. Giesz, L. De Santis, J. C. Loredano, M. P. Almeida, G. Hornecker, S. L. Protopopidis, T. Grange, C. Anton, J. Demory *et al.*, Near-optimal single-photon sources in the solid state, *Nat. Photon.* **10**, 340 (2016).
- [11] M. Lasota, R. Filip, and V. C. Usenko, Sufficiency of quantum non-gaussianity for discrete-variable quantum key distribution over noisy channels, *Phys. Rev. A* **96**, 012301 (2017).
- [12] A. Dousse, J. Suffczynski, A. Beveratos, O. Krebs, A. Lemaître, I. Sagnes, J. Bloch, P. Voisin, and P. Senellart, Ultrabright source of entangled photon pairs, *Nature (London)* **466**, 217 (2010).
- [13] J. R. A. Müller, R. M. Stevenson, J. Skiba-Szymanska, G. Shooter, J. Huwer, I. Farrer, D. A. Ritchie, and A. J. Shields, Active reset of a radiative cascade for entangled-photon generation beyond the continuous-driving limit, *Phys. Rev. Res.* **2**, 043292 (2020).
- [14] A. Fognini, A. Ahmadi, M. Zeeshan, J. T. Fokkens, S. J. Gibson, N. Sherlekar, S. J. Daley, D. Dalacu, P. J. Poole, K. D. Jöns *et al.*, Dephasing free photon entanglement with a quantum dot, *ACS Photon.* **6**, 1656 (2019).
- [15] K. A. Fischer, L. Hanschke, M. Kremser, J. J. Finley, K. Müller, and J. Vučković, Pulsed rabi oscillations in quantum two-level systems: Beyond the area theorem, *Quantum Sci. Technol.* **3**, 014006 (2018).
- [16] L. Hanschke, K. A. Fischer, S. Appel, D. Lukin, J. Wierzbowski, S. Sun, R. Trivedi, J. Vučković, J. J. Finley, and K. Müller, Quantum dot single-photon sources with ultra-low multi-photon probability, *Npj Quantum Inf.* **4**, 43 (2018).
- [17] L. Schweickert, K. D. Jöns, K. D. Zeuner, S. F. Covre da Silva, H. Huang, T. Lettner, M. Reindl, J. Zichi, R. Trotta, A. Rastelli *et al.*, On-Demand generation of background-free single photons from a solid-state source, *Appl. Phys. Lett.* **112**, 093106 (2018).

- [18] M. B. Rota, F. B. Basset, D. Tedeschi, and R. Trotta, Entanglement teleportation with photons from quantum dots: Toward a solid-state based quantum network, *IEEE J. Sel. Top. Quantum Electron.* **26**, 1 (2020).
- [19] Ch. Heyn, A. Stemmann, T. Köppen, Ch. Strelow, T. Kipp, M. Grave, S. Mendach, and W. Hansen, Highly uniform and strain-free GaAs quantum dots fabricated by filling of self-assembled nanoholes, *Appl. Phys. Lett.* **94**, 183113 (2009).
- [20] S. F. Covre da Silva, G. Undeutsch, B. Lehner, S. Manna, T. M. Krieger, M. Reindl, C. Schimpf, R. Trotta, and A. Rastelli, GaAs quantum dots grown by droplet etching epitaxy as quantum light sources, *Appl. Phys. Lett.* **119**, 120502 (2021).
- [21] D. Huber, M. Reindl, S. F. Covre da Silva, C. Schimpf, J. Martín-Sánchez, H. Huang, G. Piredda, J. Edlinger, A. Rastelli, and R. Trotta, Strain-Tunable GaAs Quantum Dot: A Nearly Dephasing-Free Source Of Entangled Photon Pairs on Demand, *Phys. Rev. Lett.* **121**, 033902 (2018).
- [22] F. Basso Basset, M. B. Rota, C. Schimpf, D. Tedeschi, K. D. Zeuner, S. F. Covre da Silva, M. Reindl, V. Zwiller, K. D. Jöns, A. Rastelli *et al.*, Entanglement Swapping with Photons Generated on Demand by a Quantum Dot, *Phys. Rev. Lett.* **123**, 160501 (2019).
- [23] K. Brunner, G. Abstreiter, G. Böhm, G. Tränkle, and G. Weimann, Sharp-Line Photoluminescence and Two-Photon Absorption of Zero-Dimensional Biexcitons in a GaAs/AlGaAs Structure, *Phys. Rev. Lett.* **73**, 1138 (1994).
- [24] S. Stuffer, P. Machnikowski, P. Ester, M. Bichler, V. M. Axt, T. Kuhn, and A. Zrenner, Two-photon Rabi oscillations in a single  $\text{In}_x\text{Ga}_{1-x}\text{As}/\text{GaAs}$  quantum dot, *Phys. Rev. B* **73**, 125304 (2006).
- [25] H. S. Nguyen, G. Sallen, M. Abbarchi, R. Ferreira, C. Voisin, P. Roussignol, G. Cassabois, and C. Diederichs, Photoneutralization and slow capture of carriers in quantum dots probed by resonant excitation spectroscopy, *Phys. Rev. B* **87**, 115305 (2013).
- [26] L. Zhai, M. C. Löbl, G. N. Nguyen, J. Ritzmann, A. Javadi, C. Spinnler, A. D. Wieck, A. Ludwig, and R. J. Warburton, Low-Noise GaAs Quantum Dots for Quantum Photonics, *Nat. Commun.* **11**, 4745 (2020).
- [27] C. Schimpf, M. Santanu, S. F. Covre da Silva, M. Aigner, and A. Rastelli, Entanglement-based quantum key distribution with a blinking-free quantum dot operated at a temperature up to 20 K, *Adv. Photon.* **3**, 065001 (2021).
- [28] A. J. Hudson, R. M. Stevenson, A. J. Bennett, R. J. Young, C. A. Nicoll, P. Atkinson, K. Cooper, D. A. Ritchie, and A. J. Shields, Coherence of an Entangled Exciton-Photon State, *Phys. Rev. Lett.* **99**, 266802 (2007).
- [29] See Supplemental Material at <http://link.aps.org/supplemental/10.1103/PhysRevB.106.L241402> for the role of normalization for the second-order autocorrelation function, modeling the multiphoton emission, power dependent blinking dynamics, and the setup efficiency.
- [30] D. Huber, M. Reindl, Y. Huo, H. Huang, J. S. Wildmann, O. G. Schmidt, A. Rastelli, and R. Trotta, Highly indistinguishable and strongly entangled photons from symmetric GaAs quantum dots, *Nat. Commun.* **8**, 15506 (2017).
- [31] F. Basso Basset, F. Salusti, L. Schweickert, M. B. Rota, D. Tedeschi, S. F. Covre da Silva, E. Rocca, V. Zwiller, K. D. Jöns, A. Rastelli *et al.*, Quantum teleportation with imperfect quantum dots, *Npj Quantum Inf.* **7**, 7 (2021).
- [32] D. F. V. James, P. G. Kwiat, W. J. Munro, and A. G. White, Measurement of qubits, *Phys. Rev. A* **64**, 052312 (2001).
- [33] E. Waks, C. Santori, and Y. Yamamoto, Security aspects of quantum key distribution with sub-Poisson light, *Phys. Rev. A* **66**, 042315 (2002).
- [34] P. Grünwald, Effective second-order correlation function and single-photon detection, *New J. Phys.* **21**, 093003 (2019).
- [35] T. Kuroda, T. Belhadj, M. Abbarchi, C. Mastrandrea, M. Gurioli, T. Mano, N. Ikeda, Y. Sugimoto, K. Asakawa, N. Koguchi *et al.*, Bunching visibility for correlated photons from single GaAs quantum dots, *Phys. Rev. B* **79**, 035330 (2009).
- [36] C. Hopfmann, W. Nie, N. L. Sharma, C. Weigelt, F. Ding, and O. G. Schmidt, Maximally entangled and gigahertz-clocked on-demand photon pair source, *Phys. Rev. B* **103**, 075413 (2021).
- [37] J.-P. Jahn, M. Munsch, L. Beguin, A. V. Kuhlmann, M. Renggli, Y. Huo, F. Ding, R. Trotta, M. Reindl, O. G. Schmidt *et al.*, An artificial Rb atom in a semiconductor with lifetime-limited linewidth, *Phys. Rev. B* **92**, 245439 (2015).
- [38] K. A. Fischer, L. Hanschke, J. Wierzbowski, T. Simmet, C. Dory, J. J. Finley, J. Vučković, and K. Müller, Signatures of two-photon pulses from a quantum two-level system, *Nat. Phys.* **13**, 649 (2017).
- [39] H. Jayakumar, A. Predojević, T. Kauten, T. Huber, G. S. Solomon, and G. Weihs, Time-bin entangled photons from a quantum dot, *Nat. Commun.* **5**, 4251 (2014).
- [40] I. Schwartz, D. Cogan, E. R. Schmidgall, Y. Don, L. Gantz, O. Kenneth, N. H. Lindner, and D. Gershoni, Deterministic generation of a cluster state of entangled photons, *Science* **354**, 434 (2016).
- [41] M. Anderson, T. Müller, J. Skiba-Szymanska, A. B. Krysa, J. Huwer, R. M. Stevenson, J. Heffernan, D. A. Ritchie, and A. J. Shields, Gigahertz-Clocked Teleportation of Time-Bin Qubits with a Quantum Dot in the Telecommunication C-Band, *Phys. Rev. Appl.* **13**, 054052 (2020).
- [42] C. Schimpf, M. Reindl, D. Huber, B. Lehner, S. F. Covre da Silva, S. Manna, M. Vyvlecka, P. Walther, and A. Rastelli, Quantum cryptography with highly entangled photons from semiconductor quantum dots, *Sci. Adv.* **7**, eabe8905 (2021).
- [43] J. Liu, R. Su, Y. Wei, B. Yao, S. F. Covre da Silva, Y. Yu, J. Iles-Smith, K. Srinivasan, A. Rastelli, J. Li *et al.*, A solid-state source of strongly entangled photon pairs with high brightness and indistinguishability, *Nat. Nanotechnol.* **14**, 6 (2019).
- [44] H. Wang, H. Hu, T.-H. Chung, J. Qin, X. Yang, J.-P. Li, R.-Z. Liu, H.-S. Zhong, Y.-M. He, X. Ding *et al.*, On-Demand Semiconductor Source of Entangled Photons Which Simultaneously Has High Fidelity, Efficiency, and Indistinguishability, *Phys. Rev. Lett.* **122**, 113602 (2019).
- [45] T. Seidelmann, C. Schimpf, T. K. Bracht, M. Cosacchi, A. Vagov, A. Rastelli, D. E. Reiter, and V. M. Axt, Two-photon excitation sets fundamental limit to entangled photon pair generation from quantum emitters, *Phys. Rev. Lett.* **129**, 193604 (2022).
- [46] S. Varoutsis, S. Laurent, P. Kramper, A. Lemaître, I. Sagnes, I. Robert-Philip, and I. Abram, Restoration of photon indistinguishability in the emission of a semiconductor quantum dot, *Phys. Rev. B* **72**, 041303(R) (2005).
- [47] M. Giustina, M. A. M. Versteegh, S. Wengerowsky, J. Handsteiner, A. Hochreiner, K. Phelan, F. Steinlechner, J. Kofler, J.-A. Larsson, C. Abellán *et al.*, Significant-Loophole-

- Free Test of Bell's Theorem with Entangled Photons, [Phys. Rev. Lett. \*\*115\*\*, 250401 \(2015\)](#).
- [48] L. K. Shalm, E. Meyer-Scott, B. G. Christensen, P. Bierhorst, M. A. Wayne, M. J. Stevens, T. Gerrits, S. Glancy, D. R. Hamel, M. S. Allman *et al.*, Strong Loophole-Free Test of Local Realism, [Phys. Rev. Lett. \*\*115\*\*, 250402 \(2015\)](#).
- [49] X.-L. Wang, L.-K. Chen, W. Li, H.-L. Huang, C. Liu, C. Chen, Y.-H. Luo, Z.-E. Su, D. Wu, Z.-D. Li *et al.*, Experimental Ten-Photon Entanglement, [Phys. Rev. Lett. \*\*117\*\*, 210502 \(2016\)](#).